

## NEUTRINO PROCESSES IN STRONG MAGNETIC FIELDS

HUAIYU DUAN

*Department of Physics  
University of California, San Diego  
La Jolla, CA 92093, USA  
E-mail: hduan@ucsd.edu*

YONG-ZHONG QIAN

*School of Physics and Astronomy  
University of Minnesota  
Minneapolis, MN 55455, USA  
E-mail: qian@physics.umn.edu*

The processes  $\nu_e + n \rightleftharpoons e^- + p$  and  $\bar{\nu}_e + p \rightleftharpoons e^+ + n$  provide the dominant mechanisms for heating and cooling the material below the stalled shock in a core-collapse supernova. We summarize the major effects of strong magnetic fields on the rates of the above reactions and illustrate these effects with a simple supernova model. Due to parity violation of weak interaction the heating rates are asymmetric even for a uniform magnetic field. The cooling rates are also asymmetric for nonuniform fields. The most dramatic effect of strong magnetic fields of  $\sim 10^{16}$  G is suppression of the cooling rates by changing the equations of state through the phase space of  $e^-$  and  $e^+$ .

### 1. Introduction

The neutrino processes

$$\nu_e + n \rightleftharpoons e^- + p, \quad (1)$$

$$\bar{\nu}_e + p \rightleftharpoons e^+ + n \quad (2)$$

play important roles in core-collapse supernovae. After the shock is stalled, neutrinos emitted from the protoneutron star exchange energy with the material below the shock mainly through these processes. The forward processes in Eqs. (1) and (2) heat the material through the absorption of  $\nu_e$  and  $\bar{\nu}_e$ , while the reverse processes cool the material by emitting them. In the neutrino-driven supernova mechanism [1], the competition between heating and cooling of the material by these processes is expected to result

in net energy gain for the stalled shock, which is then revived to make a successful supernova explosion. Unfortunately, the current consensus is that this mechanism does not work in spherically symmetric models [2, 3]. On the other hand, strong magnetic fields may be generated during the formation of protoneutron stars and in turn affect supernova dynamics. Observations have shown that some neutron stars possess magnetic fields as strong as  $\sim 10^{15}$  G [4–6]. Although it is not clear how strong magnetic fields in supernovae could be, some calculations indicate that fields of  $10^{15}$ – $10^{16}$  G are not impossible [7]. While strong magnetic fields can affect supernova dynamics in many possible ways, here we consider their effects on the neutrino processes. Because the explosion energy is much smaller than the gravitational binding energy of the protoneutron star and nearly all of the latter is released in neutrinos, it is natural to expect that a small change in the neutrino physics input may have a large impact on the supernova mechanism.

The effects of strong magnetic fields on neutrino processes have been studied in various approximations [8–15]. In our recent work, we have calculated the effects of magnetic fields on the four processes in Eqs. (1) and (2) to the 0th [16] and 1st order [17] in  $E_\nu/m_N$ , where  $E_\nu$  is the neutrino energy and  $m_N$  is the nucleon mass. Here we summarize our results and list some issues that remain to be addressed.

## 2. Neutrino Processes in Strong Magnetic Fields

### 2.1. General Effects of Magnetic Fields

An obvious effect of the magnetic field is polarization of the spin of a nonrelativistic nucleon. When this effect is small, the polarization of the nucleon spin may be written as

$$\chi \simeq \frac{\mu B}{T} = 3.15 \times 10^{-2} \left( \frac{\mu}{\mu_N} \right) \left( \frac{B}{10^{16} \text{ G}} \right) \left( \frac{\text{MeV}}{T} \right), \quad (3)$$

where  $\mu$  is the nucleon magnetic moment,  $\mu_N = e/2m_p$  is the nuclear magneton,  $B$  is the magnetic field strength, and  $T$  is the gas temperature. Due to parity violation of weak interaction polarization of the nucleon spin introduces a dependence on the angle  $\Theta_\nu$  between the directions of the neutrino momentum and the magnetic field for the cross sections of the forward processes in Eqs. (1) and (2) (see Sec. 2.2) and for the differential volume reaction rates of the reverse processes (see Sec. 2.3).

In addition, assuming a magnetic field in the positive  $z$ -direction, the motion of a proton in the  $xy$ -plane is quantized into Landau levels (see

e.g. Ref. [18]) with kinetic energies

$$E_p(n_p, k_{pz}) = \frac{k_{pz}^2}{2m_p} + \left(n_p + \frac{1}{2}\right) \frac{eB}{m_p}, \quad n_p = 0, 1, 2, \dots, \quad (4)$$

where  $n_p$  is the quantum number of the proton Landau level and  $k_{pz}$  is the  $z$ -component of the proton momentum. We are interested in gas temperatures of  $T \gtrsim 1$  MeV and magnetic fields of  $B \sim 10^{16}$  G. As  $eB/m_p = 63(B/10^{16} \text{ G}) \text{ keV}$ , for such conditions a proton is able to occupy Landau levels with  $n_p \gg 1$  and can be considered as classical.

For the conditions of interest here,  $e^-$  and  $e^+$  are relativistic. Their Landau levels have energies

$$E_e(n_e, k_{ez}) = \sqrt{m_e^2 + k_{ez}^2 + 2n_e eB}, \quad (5)$$

where symbols are defined similarly to those for the proton. The above equation has taken spin into account. Note that the  $e^-$  or  $e^+$  in the ground Landau level ( $n_e = 0$ ) has only one spin state. This introduces an additional dependence on  $\Theta_\nu$  (independent of polarization of the nucleon spin) for the cross sections of the forward processes in Eqs. (1) and (2) (see Sec. 2.2) and for the differential volume reaction rates of the reverse processes (see Sec. 2.3). The effects of Landau levels are more prominent for  $e^-$  and  $e^+$  than for nucleons. This can be seen from the quantum number for the highest Landau level occupied by  $e^-$  or  $e^+$  with energy  $E_e$ ,

$$(n_e)_{\max} = \left[ \frac{E_e^2 - m_e^2}{2eB} \right]_{\text{int}} = \left[ 8.45 \times 10^{-3} \left( \frac{E_e^2 - m_e^2}{\text{MeV}^2} \right) \left( \frac{10^{16} \text{ G}}{B} \right) \right]_{\text{int}}. \quad (6)$$

To account for the effects of Landau levels, part of the integration over the phase space of  $e^-$  or  $e^+$  is changed to a summation over possible Landau levels, i.e.

$$2 \int \frac{d^3 k_e}{(2\pi)^3} \rightarrow \frac{eB}{2\pi} \sum_{n_e=0}^{(n_e)_{\max}} g_{n_e} \int \frac{dk_{ez}}{2\pi}, \quad (7)$$

where  $g_{n_e}$  is the number of spin states for the  $n_e$ th Landau level ( $g_{n_e} = 1$  for  $n_e = 0$  and 2 for  $n_e > 0$ ).

## 2.2. Heating Processes

To the 0th order in  $E_\nu/m_N$ , the cross sections of the forward processes in Eqs. (1) and (2) are found to be [16]

$$\begin{aligned} \sigma_{\nu N}^{(0,B)} = & \sigma_{B,1} \left[ 1 + 2\chi \frac{(f \pm g)g}{f^2 + 3g^2} \cos \Theta_\nu \right] \\ & + \sigma_{B,2} \left[ \frac{f^2 - g^2}{f^2 + 3g^2} \cos \Theta_\nu + 2\chi \frac{(f \mp g)g}{f^2 + 3g^2} \right], \end{aligned} \quad (8)$$

where the energy-dependent factors  $\sigma_{B,1}$  and  $\sigma_{B,2}$  are defined as

$$\sigma_{B,1} = \frac{G_F^2 \cos^2 \theta_C}{2\pi} (f^2 + 3g^2) \epsilon B \sum_{n_e=0}^{(n_e)_{\max}} \frac{g_{n_e} E_e}{\sqrt{E_e^2 - m_e^2 - 2n_e \epsilon B}}, \quad (9)$$

$$\sigma_{B,2} = \frac{G_F^2 \cos^2 \theta_C}{2\pi} (f^2 + 3g^2) \epsilon B \frac{E_e}{\sqrt{E_e^2 - m_e^2}}, \quad (10)$$

with  $E_e = E_\nu \pm \Delta$  and  $\Delta$  being the neutron-proton mass difference. In the above equations, the upper sign is for  $\nu_e$  absorption on  $n$  and the lower sign for  $\bar{\nu}_e$  absorption on  $p$ .

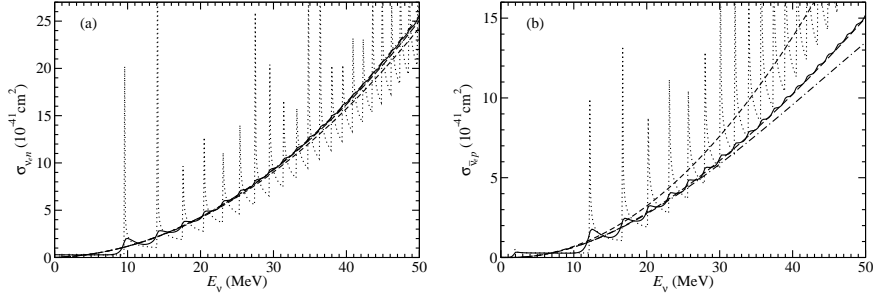


Figure 1. The cross sections of  $\nu_e + n \rightarrow e^- + p$  (a) and  $\bar{\nu}_e + p \rightarrow e^+ + n$  (b) as functions of neutrino energy  $E_\nu$ . The angle  $\Theta_\nu$  between the directions of the neutrino momentum and the magnetic field is taken to be 0. The dotted and solid curves are the cross sections to the 0th and 1st order in  $E_\nu/m_N$ , respectively. Both assume a magnetic field of  $B = 10^{16}$  G. In addition, the solid curves assume a temperature  $T = 2$  MeV for the nucleon gas. The short-dashed and dot-dashed curves are the cross sections to the 0th and 1st order in  $E_\nu/m_N$ , respectively, but for  $B = 0$ . The long-dashed curve in (b) is for  $B = 0$  and includes some corrections beyond the 1st order. The differences between the short-dashed, dot-dashed, and long-dashed curves in (b) at the high-energy end are mostly due to the combined effects of nucleon recoil and weak magnetism.

Comparing  $\sigma_{B,1}$  with the well-known expression for the 0th-order cross

section in the absence of magnetic fields,

$$\sigma_{\nu N}^{(0)} = \frac{G_F^2 \cos^2 \theta_C}{\pi} (f^2 + 3g^2) k_e E_e, \quad (11)$$

one can see that the only difference is the change in phase space [see Eq. (7)]. To illustrate the effects of strong magnetic fields, we plot the cross sections of neutrino absorption on nucleons for  $B = 10^{16}$  G and 0 in Fig. 1 (see Ref. [17] for more details). An immediate observation is that the cross sections are enhanced (dotted curves in Fig. 1) if the energy of the outgoing  $e^-$  or  $e^+$  satisfies the condition

$$E_e = \sqrt{m_e^2 + 2n_e e B} \quad (12)$$

for  $n_e > 0$ . This is because a new Landau level opens up when Eq. (12) is satisfied. Just as discrete energy levels of atoms lead to absorption lines in the light spectra, ideally the presence of strong magnetic fields would produce sharp dips in the neutrino energy spectra where Eq. (12) holds. However, the nucleons absorbing neutrinos have thermal motion, which will smear out these sharp dips. We have included the thermal motion of nucleons and calculated the cross sections to the 1st order in  $E_\nu/m_N$  [17]. Even for magnetic fields as strong as  $10^{16}$  G, the thermal motion of nucleons with  $T \sim 2$  MeV is enough to smooth out almost all the spikes in  $\sigma_{\nu N}(E_\nu)$  (see solid curves in Fig. 1). The effect of the magnetic field is further diminished by averaging the cross sections over neutrino energy spectra. A magnetic field of  $10^{16}$  G causes changes of only a few percent to the average cross sections.

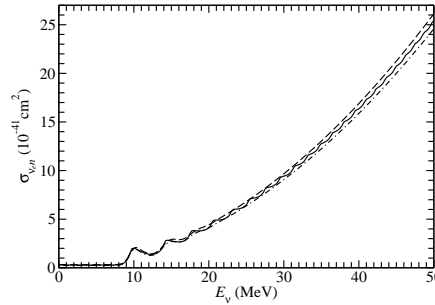


Figure 2. The cross section of  $\nu_e + n \rightarrow e^- + p$  to the 1st order in  $E_\nu/m_N$  for  $B = 10^{16}$  G and  $T = 2$  MeV. The angle  $\Theta_\nu$  between the directions of  $\nu_e$  and the magnetic field is taken to be 0 (dot-dashed curve),  $\pi/2$  (solid curve), and  $\pi$  (dashed curve), respectively.

The term proportional to  $\sigma_{B,1}$  in Eq. (8) depends on the direction of the incoming neutrino with respect to the magnetic field. This is due to parity violation of weak interaction. In fact, as long as the target nucleon has a polarization  $\chi$ , the lowest-order expression of the cross section in the absence of magnetic fields can be written as

$$\sigma_{\nu N}^{(0)}(\chi) = \sigma_{\nu N}^{(0)} \left[ 1 + 2\chi \frac{(f \pm g)g}{f^2 + 3g^2} \cos \Theta_\nu \right], \quad (13)$$

which has exactly the same angular dependence as the  $\sigma_{B,1}$  term in Eq. (8). The appearance of the term proportional to  $\sigma_{B,2}$  in this equation is due to the fact that there is only one spin state for the ground Landau level of  $e^-$  or  $e^+$ . This term has an angular dependence even if the nucleon polarization  $\chi = 0$ . Nevertheless, this dependence is again due to parity violation as the  $e^-$  or  $e^+$  in the ground Landau level is polarized. For crude estimates of the angular dependence, we use Eq. (13). As the nucleon form factors  $f = 1$  and  $g = 1.26$  are close in numerical value,  $\sigma_{\nu ep}^{(0)}(\chi_p)$  has little dependence on  $\Theta_\nu$ . On the other hand, the  $\Theta_\nu$ -dependent term for  $\sigma_{\nu en}^{(0)}(\chi_n)$  is  $\sim \chi_n \cos \Theta_\nu$ . The angular dependence of  $\sigma_{\nu en}$  for a strong magnetic field of  $B = 10^{16}$  G and a gas temperature of  $T = 2$  MeV is shown in Fig. 2.

### 2.3. Cooling Processes

Because  $e^-$  and  $e^+$  do not have definite velocities [18], we define a volume reaction rate  $\Gamma_{eN}$ , which gives the rate of e.g.,  $e^+$  capture per neutron when multiplied by the  $e^+$  number density  $n_{e^+}$ . The differential volume reaction rates to the 0th order in  $E_\nu/m_N$  are found to be [16]

$$\begin{aligned} \frac{d\Gamma_{eN}^{(0,B)}}{d \cos \Theta_\nu} &= \frac{\Gamma_{eN}^{(0)}}{2} \left[ 1 + 2\chi \frac{(f \pm g)g}{f^2 + 3g^2} \cos \Theta_\nu \right] \\ &+ \delta_{n_e,0} \frac{\Gamma_{eN}^{(0)}}{2} \left[ \frac{f^2 - g^2}{f^2 + 3g^2} \cos \Theta_\nu + 2\chi \frac{(f \mp g)g}{f^2 + 3g^2} \right], \end{aligned} \quad (14)$$

where

$$\Gamma_{eN}^{(0)} = \frac{G_F^2 \cos^2 \theta_C}{2\pi} (f^2 + 3g^2) E_\nu^2 \quad (15)$$

with  $E_\nu = E_e \pm \Delta$  is the volume reaction rate in the absence of magnetic fields. In the above equations, the upper sign is for  $e^+$  capture on  $n$  and the lower sign for  $e^-$  capture on  $p$ . The angular dependence for neutrino emission in Eq. (14) is the same as that for neutrino absorption in Eq. (8) and is due to parity violation of weak interaction as explained in Sec. 2.2.

However, the volume reaction rates for the cooling processes obtained by integrating the differential rates in Eq. (14) over  $\Theta_\nu$  are isotropic for a uniform magnetic field. This is in contrast to the cross sections in Eq. (8) for the heating processes.

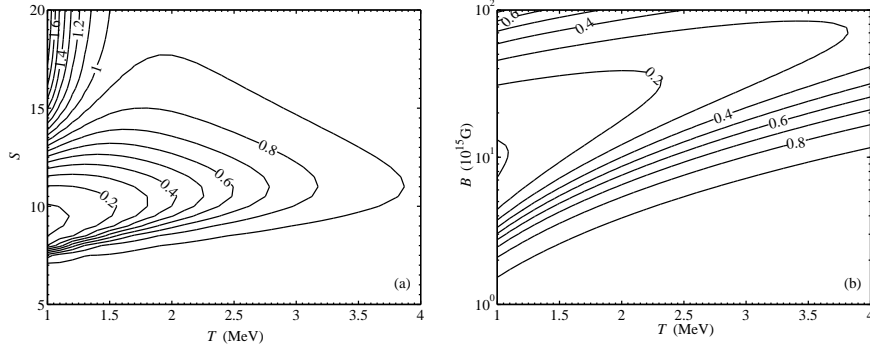


Figure 3. Contours of the ratio of the total cooling rate with magnetic fields to that without. A magnetic field of  $10^{16}$  G is assumed for (a) and a total entropy per nucleon  $S = 10$  is assumed for (b). A constant electron fraction  $Y_e = 0.5$  is assumed for both.

Like the cross sections for the heating processes, the volume reaction rates of the cooling processes are not much affected even for magnetic fields as strong as  $10^{16}$  G. However, the cooling rates could be severely suppressed by such strong magnetic fields due to changes in the equations of state through the phase space of  $e^-$  and  $e^+$  [16]. Given the electron fraction  $Y_e$ , the total entropy per nucleon  $S$ , and the gas temperature  $T$ , one can solve the equations of state

$$\frac{\rho Y_e}{m_N} = \mathbf{n}_{e^-} - \mathbf{n}_{e^+}, \quad (16)$$

$$S = S_N + S_\gamma + S_{e^-} + S_{e^+}, \quad (17)$$

to obtain the baryon mass density  $\rho$  and the electron degeneracy parameter  $\eta_e$  for cases of strong and no magnetic fields. The cooling rates (per nucleon) in each case can then be calculated by integrating the volume reaction rates over the energy-differential number densities of  $e^-$  and  $e^+$ . The suppression of the total cooling rate by strong magnetic fields is shown in Fig. 3. The reason for this suppression is that compared with the case of no magnetic fields, there are more low-energy  $e^-$  and  $e^+$  in magnetic fields of  $\sim 10^{16}$  G as most of the  $e^-$  and  $e^+$  reside in the ground Landau level ( $n_e = 0$ ).

### 3. Application to Core-Collapse Supernovae

To illustrate the effects of strong magnetic fields on supernova dynamics, we consider a simple supernova model. All neutrinos are assumed to be emitted at the same radius  $R_\nu = 50$  km. The shock is stalled at a radius  $R_s = 200$  km. The electron fraction and the total entropy per nucleon are taken to be  $Y_e = 0.5$  and  $S = 10$ , respectively, and held constant between  $R_\nu$  and  $R_s$ . We adopt the temperature profile

$$T(r) = T(R_\nu) \frac{R_\nu}{r} = 4 \left( \frac{50 \text{ km}}{r} \right) \text{ MeV}. \quad (18)$$

With the above assumptions, we calculate the total heating and cooling rates as functions of radius  $r$  for cases of strong and no magnetic fields [the equations of state (16) and (17) are solved to obtain  $\rho$  and  $\eta_e$  for calculating the total cooling rate in both cases]. In the absence of magnetic fields, the total heating rate is found to be equal to the total cooling rate at a gain radius  $R_g = 137$  km, above which heating dominates cooling.

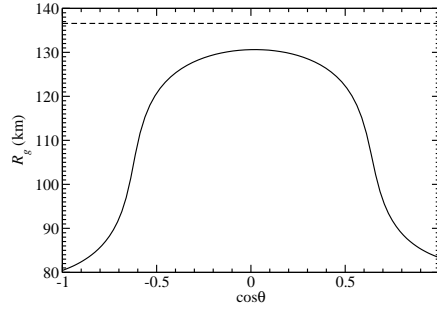


Figure 4. The gain radius  $R_g$  as a function of  $\cos \theta$  (solid curve) for a dipole magnetic field. Compared with the case for  $B = 0$  (dashed curve), the gain radius is substantially reduced at the north and south poles where the magnetic fields are the strongest.

Consider a magnetic field of dipole configuration in spherical coordinates  $(r, \theta, \phi)$ ,

$$\mathbf{B} = B_0 \left( \frac{R_\nu}{r} \right)^3 (2 \cos \theta \hat{\mathbf{r}} + \sin \theta \hat{\boldsymbol{\theta}}). \quad (19)$$

We calculate  $R_g$  for  $B_0 = 5 \times 10^{16}$  G and plot it as a function of  $\cos \theta$  in Fig. 4. Due to suppression of the cooling rates by strong magnetic fields,  $R_g$  becomes smaller in the presence of strong magnetic fields compared with the



case of no magnetic fields. As a result, there is more region of net heating below the stalled shock and the neutrino-driven supernova mechanism may work more efficiently. The cooling rates are most suppressed at north and south poles where the magnetic fields are the strongest. The stalled shock is likely to be revived earlier and more energetically in these directions. It is also worth mentioning that there is a small difference in the gain radius between the north and south poles (see Fig. 4). This is due to the angular dependence of the heating processes discussed in Sec. 2.2. This small asymmetry may result in a kick to the protoneutron star that could explain the space velocities observed for pulsars.

#### 4. Open Issues

Although we have demonstrated that strong magnetic fields have important effects on the dynamics of core-collapse supernovae, our results depend on how strong the magnetic fields in supernovae could be. This is the biggest open issue. Alternatively, our results can be used to gauge whether magnetic fields would affect supernova dynamics by changing the rates of neutrino processes. In this regard, we find that magnetic fields weaker than  $10^{15}$  G would have negligible effects on the neutrino processes, while fields of  $\sim 10^{16}$  G would dramatically change supernova dynamics through neutrino physics. Of course, magnetic fields weaker than  $10^{15}$  G may already have important hydrodynamic effects in supernovae. This is not considered here but should be investigated by future studies. Another open issue is how to model supernova explosions by including both hydrodynamic effects and changes in the neutrino processes due to strong magnetic fields of  $\sim 10^{16}$  G. The processes  $\nu_e + n \rightarrow e^- + p$  and  $\bar{\nu}_e + p \rightarrow e^+ + n$  not only provide the dominant mechanisms for heating the material below the stalled shock, but also are the main opacity sources for determining the thermal decoupling of  $\nu_e$  and  $\bar{\nu}_e$  from the protoneutron star, and hence, their emission energy spectra. An interesting issue is whether strong magnetic fields in supernovae could leave detectable imprints on the neutrino energy spectra.

#### Acknowledgements

HD is very grateful to the hospitality of Tony Mezzacappa, George M. Fuller, and the Institute for Nuclear Theory during the workshop. He also wants to thank Arkady Vainshtein for helpful discussions. This work was supported in part by DOE grant DE-FG02-87ER40328.

## References

1. H. A. Bethe and J. R. Wilson, *Astrophys. J.* **295**, 14 (1985).
2. M. Rampp and H.-T. Janka, *Astrophys. J.* **539**, L33 (2000), astro-ph/0005438.
3. M. Liebendörfer, A. Mezzacappa, F.-K. Thielemann, O. E. Messer, W. R. Hix, and S. W. Bruenn, *Phys. Rev.* **D63**, 103004 (2001), astro-ph/0006418.
4. C. Kouveliotou, T. Strohmayer, K. Hurley, J. van Paradijs, M. H. Finger, S. Dieters, P. Woods, C. Thompson, and R. C. Duncan, *Astrophys. J.* **510**, L115 (1999), astro-ph/9809140.
5. E. V. Gotthelf, G. Vasisht, and T. Dotani, *Astrophys. J.* **522**, L49 (1999), astro-ph/9906122.
6. A. I. Ibrahim, J. H. Swank, and W. Parke, *Astrophys. J.* **584**, L17 (2003), astro-ph/0210515.
7. S. Akiyama, J. C. Wheeler, D. L. Meier, and I. Lichtenstadt, *Astrophys. J.* **584**, 954 (2003), astro-ph/0208128.
8. E. Roulet, *JHEP* **01**, 013 (1998), hep-ph/9711206.
9. L. B. Leinson and A. Pérez, *JHEP* **9809**, 020 (1998), astro-ph/9711216.
10. D. Lai and Y.-Z. Qian, *Astrophys. J.* **505**, 844 (1998), astro-ph/9802345.
11. P. Arras and D. Lai, *Phys. Rev.* **D60**, 043001 (1999), astro-ph/9811371.
12. A. A. Gvozdev and I. S. Ognev, *JETP Lett* **69**, 365 (1999), astro-ph/9909154.
13. D. Chandra, A. Goyal, and K. Goswami, *Phys. Rev.* **D65**, 053003 (2002), hep-ph/0109057.
14. C. J. Horowitz, *Phys. Rev.* **D65**, 043001 (2002), astro-ph/0109209.
15. K. Bhattacharya and P. B. Pal, *Pramana* **62**, 1041 (2004), hep-ph/0209053.
16. H. Duan and Y.-Z. Qian, *Phys. Rev.* **D69**, 123004 (2004), astro-ph/0401634.
17. H. Duan and Y.-Z. Qian (2005) (to be submitted to Phys. Rev. D). ([astro-ph/0506033](#))
18. L. D. Landau and E. M. Lifshitz, *Quantum Mechanics: non-relativistic theory* (Pergamon, Oxford, 1977), 3rd ed.